New asteroseismic analysis of the subdwarf B pulsator PG 1219+534

Marie-Julie Péters[1], Valérie Van Grootel[1], Marc-Antoine Dupret[1], Elizabeth M.Green[2] Gilles Fontaine[3], Stéphane Charpinet[4], Pierre Brassard[3]

[1] Université de Liège [2] The University of Arizona [3] Université de Montréal [4] Université de Toulouse

Introduction

We present a new asteroseismic modeling of the short-period sdB pulsator PG 1219+534, based on the most recent stellar models (third generation) and new observations during a 6-month campaign in Arizona. Considering the spectroscopic analysis and mode identification from observed rotational multiplets, the best-fit third generation model is isolated matching the observed and computed periods with an average dispersion of 0.5%. We compared our results with the previous work by Charpinet et al. (2005) that used the second generation models. Moreover, by the presence of a fine structure (frequency multiplets), we tried also to characterize the rotation and determine the rotation rate of the surface and the core of the star. Finally, we derived properties on the convective core from evolutionary tracks.

Observations

We derived the atmospheric parameters from high S/N low and medium resolution spectroscopy modeling and we obtained $T_{\rm eff} = 34258 \pm 170\,{\rm K}$ and $\log g = 5.838 \pm 0.030$.

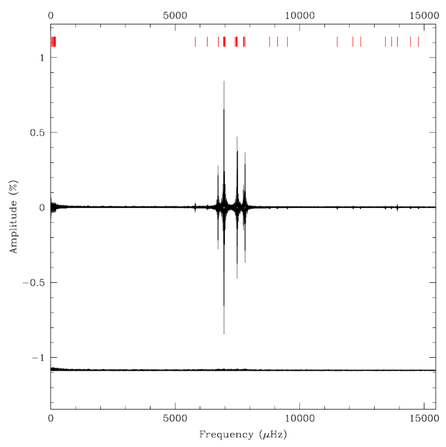

Figure 1

During an observation campaign spreading over 6 months in 2007, photometric data were obtained with the Mont4kccd on Steward Observatory's 1.55-m Mt. Bigelow telescope in Arizona. To extract the frequencies, a Fourier analysis and prewhitening techniques were applied to the total light curve. The Fourier Transform of the Mt Bigelow data is showed on the **Figure 1.**

Table 1 lists the 9 oscillation p–modes extracted (in bold) and their associated rotational multiplets.

Id.	P_{obs}(s)	P_{th}(s)	Amplitude (%)	l	k
f_{001}	**143.650**	**144.281**	0.837	1	2
f_{005}	133.510	-	0.291	-	-
f_{002}	**133.521**	**133.565**	0.392	2	2
f_{006}	133.532	-	0.266	-	-
f_{037}	128.073	-	0.020	-	-
f_{003}	**128.078**	**129.176**	0.375	1	3
f_{030}	128.083	-	0.024	-	-
f_{004}	**148.777**	**148.885**	0.304	4	1
f_{042}	158.784	-	0.016	-	-
f_{041}	**158.791**	**158.870**	0.016	0	1
f_{007}	**129.093**	**129.142**	0.157	4	2
f_{022}	**172.220**	**172.188**	0.031	2	0
f_{056}	**82.336**	**82.668**	0.009	2	6
f_{053}	**86.869**	**85.231**	0.010	1	8

Table 1

Methods

The forward method for asteroseismology is applied and requires a double-optimization procedure.

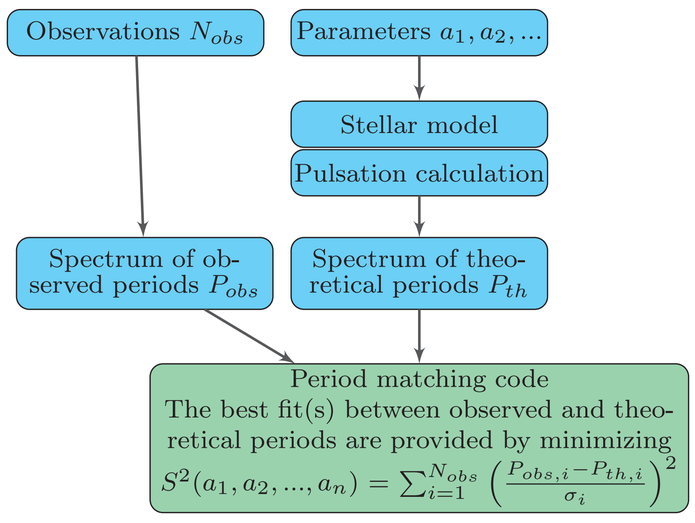

The asteroseismic analysis is based of third generation (3G) of sdB stellar models that are complete, in order to determine the structural parameters and the properties of the core. Four parameters are required: the total mass of the star M_*, the mass contained in the hydrogen-rich envelope $\log(M_{\rm env}/M_*)$, the mass contained in the core $\log(M_{\rm core}/M_*)$ and the chemical composition of the core $X({\rm He}) + X({\rm C+O}) = 1$.

Reference

[1] Charpinet, S., Fontaine, G., Brassard, P., Green, E. M., & Chayer, P. 2005, A&A, 437, 575

Asteroseismic analysis

Figure 2: Map of the S^2 in the $\log {\rm q(H)} - M_*$ plane

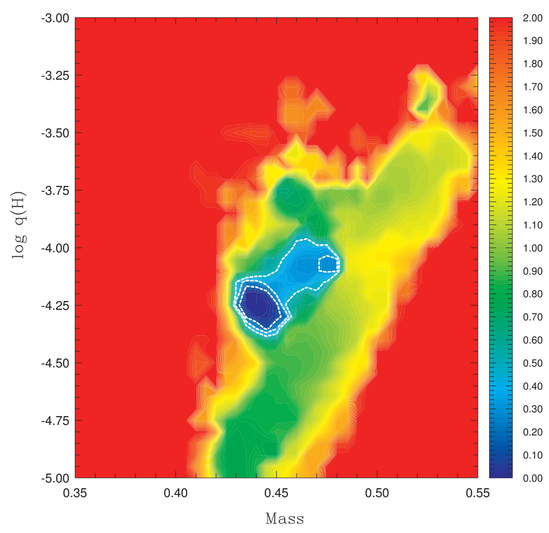

Figure 3: Map of the S^2 in the $X_{\rm core}(C+O) - \log {\rm q(core)}$ plane

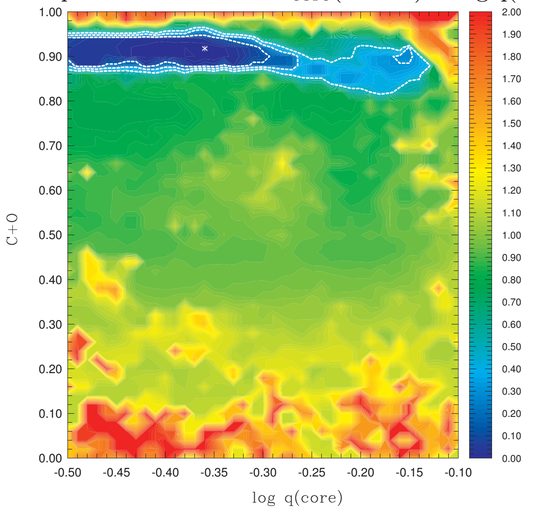

Considering the spectroscopic analysis and mode identification from observed rotational multiplets, the optimization code spotted a region of parameter space corresponding to minimum of the merit function ($S^2 \sim 0.618$). This region is represented on the **Figures 2 and 3** showing the maps of the S^2 function around the optimal model solution. The location of this optimal model in the maps is indicated by a cross and its structural parameters are presented in the **Table 2**.

Parameter	Asteroseismology	
	2G model (Charpinet et al. 2005)	3G model
$T_{\rm eff}$(K)	33640 ± 1360	34200 ± 375
$\log g$	5.807 ± 0.006	5.806 ± 0.003
$M_*/M_\odot$	0.421 ± 0.007	0.441 ± 0.004
$\log(M_{\rm env}/M_*)$	-4.517 ± 0.090	-4.250 ± 0.040
$\log(M_{\rm core}/M*)$	-	$-0.370^{+0.030}_{-0.060}$
$X_{\rm core}(C+O)$	-	0.905 ± 0.020
$R_*/R_\odot$	0.135 ± 0.003	0.1378 ± 0.0009
$L_*/L_\odot$	22.43 ± 1.16	$22.38^{+1.95}_{-0.30}$

Table 2

On the figures, as shown on the right color scale, the areas of the plots fill with dark blue represent the good fit between the observed and theoretical periods. White contours show regions where the period fits have S^2 values within the 1σ, 2σ and 3σ confidence levels relative to the best-fit solution. **Figure 3** shows an elongated valley along the $\log q$(core) parameter that reflects the fact that p–modes observed are not sensitive to the stellar innermost layers, and therefore the size of the core cannot constrained. The core composition is, however, indirectly constrained and we can note that the star is already at an evolved stage: 91% of helium is consumed in the core.

Aspects of the rotation

Figure 4

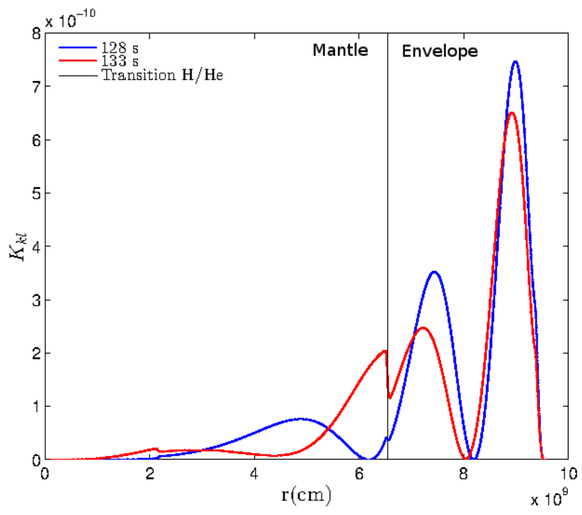

The stellar rotation leads to a rotational splitting of non-radial modes with $m = 0$ into their $2l+1$ components. At first order of approximation, this splitting creates groups of evenly spaced multiplets in the frequency domain. Assuming an internal rotation law $\omega(r)$, the frequency spacing is

$$\Delta\nu_{kl} = m \int_0^R K_{kl}(r)\omega(r)dr$$

We calculated the rotational kernels for the mode $(1,1)$ to 128 s and for the mode $(2,2)$ to 133 s in the 3G model (see **Fig 4**). We see that, below the mantle–core boundary (in black), the kernels falls quickly to low values and thus, we couldn't conclude about a differential rotation between the core and the envelope because the amplitudes of eigenfunctions are low in the core. In the case of a solid rotation, we could estimate a rotation period $P_{\rm rot} = 35.16 \pm 10.15$ days although the rotational kernels probe essentially the stellar envelope.

Evolutionary track of PG 1219+534

Figure 5

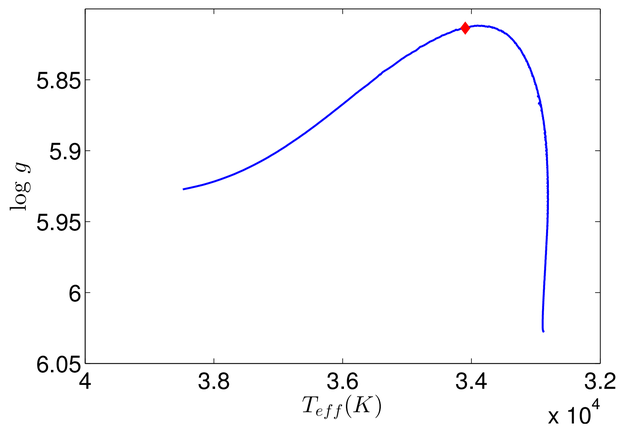

Figure 6

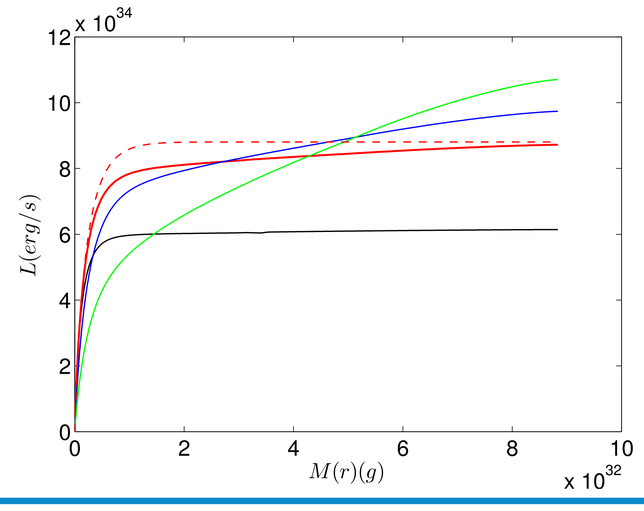

Figure 5 represents the evolutionary track of the star characterized by the values of the 3G model from the models throughout its evolution. The rise on the track on the figure to the lower surface gravity and temperatures illustrates the first phase of the combustion of helium, the star is expanding. When 80% of helium is consumed, the sdB starts to shrink under gravity effects and evolves to the higher $\log g$ and $T_{\rm eff}$. Considering the atmospheric parameters, the evolutionary model closest to the 3G optimal model is represented by a red diamond. Based on the models of this sequence, we compared the behavior of models at different evolution stages and 3G static model. For instance, the luminosity L of the sdB star as a function of depth expressed in mass fraction is represented in **Figure 6**.

- In the core, L increases rapidly due to the production of energy by the nuclear reaction.
- In the inert envelope, the slope of the luminosity increases with the evolution stage because the shrinking by the gravity contributes more and more to L.
- For the 3G model (in dashed line), L remains constant in the outer layers because only the rate of energy supply by the nuclear reaction is considered for the calculations. The 3G static model is close to the evolutionary model because the star is not already affected a lot by the shrinking at this evolved stage.
- The structural parameters of the star are similar in the 2 cases and, although the static models are much less sophisticated, they are sufficient for inferring the most important structural parameters.